

# Adaptive Beam-Steering LiDAR using a Liquid-Crystal Integrated Optical Phased Array

**Kazuki Nakamura<sup>1</sup>, Kenji Narumi<sup>1</sup>, Kohei Kikuchi<sup>1</sup>, Yumiko Kato<sup>1</sup>, Akira Hashiya<sup>1</sup>, Takaiki Nomura<sup>1</sup>, Masahiko Tsukuda<sup>1</sup>, Yoshiki Sasaki<sup>1</sup>, Kazuya Hisada<sup>1</sup> and Yasuhisa Inada<sup>1</sup>**

nakamura.kazuki@jp.panasonic.com

<sup>1</sup>Technology Division, Panasonic Holdings Co., 3-1-1 Yakumo-Nakamachi, Moriguchi-City, Osaka 570-8501, Japan

Keywords: Dynamic beam-steering, Optical phased array, Bragg-reflector waveguide, LiDAR

## ABSTRACT

We have developed an adaptive beam-steering LiDAR using a liquid-crystal tunable on-chip beam-steering device. 3D target tracking is demonstrated by aiming the beam at objects detected with a camera.

## 1 Introduction

LiDARs have already been widely used as 3D sensors to achieve simultaneous localization and mapping (SLAM) and object detection and recognition, which are essential for machine automations<sup>1</sup>. LiDARs are characterized by high resolution and wide field of view, and to realize it, a laser is swept using a beam steering device. For the beam steering device, mechanical scan<sup>2</sup>, MEMS mirror<sup>3</sup>, optical phased array (OPA)<sup>4-6</sup> and LCOS device<sup>7</sup> can be used. At present, most of commercially available LiDARs contain bulky mechanical one using motors, and LiDARs using MEMS are almost ready to be released. In general, these systems suffer from weakness to shocks and vibration due to mechanical parts and limited to periodic motion by inertia. On the other hand, OPA integrated with optical waveguide, phase shifter and antenna array can steer the light direction radiated from the antenna by the phase control. Therefore, OPA enables agile beam pointing and bring the multi-functional operation to LiDARs. The steering angle of the OPA is determined by the pitch of the antenna array. In 1D-OPA, high-density antenna arrays are realized, and large steering angles are demonstrated<sup>8,9</sup>. However, 1D-OPA requires wavelength tuning for the beam steering of the second axis<sup>6,10-11</sup>. In 2D-OPA, high-density integration of antennas is difficult<sup>5,12-13</sup>.

We have proposed a liquid crystal tunable antenna (LC-tunable antenna) that can attach a second steering axis to 1D-OPA at a fixed wavelength<sup>14</sup>. The LC-tunable antenna inspired by the structure of VECSEL supports the propagation mode of the liquid crystal core with DBR reflection. LC-tunable antennas can obtain the surface emission of the angle corresponding to the effective refractive index of the propagation mode from DBR with higher transmittance (Fig. 1). That is, the radiation angle can be changed by rotating the liquid crystal molecules in the core by the external electric field. The LC-tunable

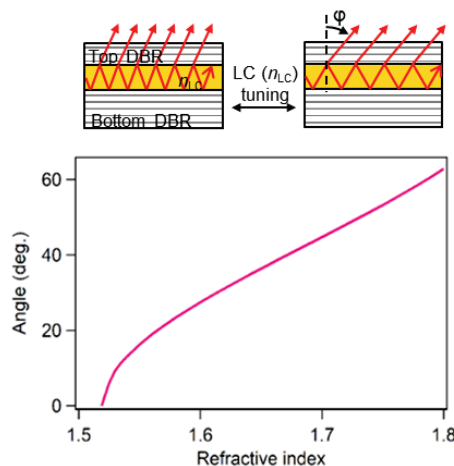


**Fig.1** Calculated angle of the output beams as a function of the refractive index of the LC.

antenna operates as a 1D beam steering device alone and as a 2D beam steering device when combined with 1D-OPA. In previous work, the 1 D beam steering of 30 ° was verified by the single LC-tunable antenna. The beam scan of 15 ° \* 16 ° was realized by incorporating into 1D-OPA<sup>14</sup>.

The LC-tunable beams steering devices not only scans the beam periodically but can also irradiate the beam in an arbitrary direction. In this report, we constructed a LiDAR prototype which recognizes an object and measures its direction by utilizing this feature.

## 2 Experiment

To realize this function, a fusion system with a visible light camera and a near infrared LiDAR was constructed. A visible light camera captures an image including a target as a video. Image processing software recognizes an object in the image for each frame of the moving image and calculates an irradiation angle of a beam. The 1D beam steering device irradiates the beam to the calculated angle. A time of flight (ToF) camera receives reflected light from an object as a ranging image. The software extracts distance information in the beam irradiation direction from the ranging image to obtain distance data of an object. As the object moves in the image, the beam also tracks and irradiates the object for distance measurement.

## 2.1 Hardware configuration

Figure 2 shows the hardware configuration of the prototype LiDAR. The center of the visible light camera's horizontal field of view (FOV) was aligned with the center of the steering angle. The horizontal viewing angle of the visible light camera was  $49.2^\circ$ , and FOV of the ToF camera was  $50^\circ(\text{H}) \times 19^\circ(\text{V})$ . The ToF camera and the laser were synchronized by the trigger signal of the illumination light of the ToF camera. The wavelength of the laser was 940 nm. The laser and the beam steering device were connected by an optical fiber. The light emitted from the beam steering device was steered horizontally. Depending on the shape of the antenna, the beam spreads vertically. Therefore, the beam was formed into the dot shape by arranging the cylindrical lens in front of the beam steering device.

The beam steering device uses a LC-tunable beam steering device with single antenna. Figure 3 shows the emission angle as a function of the applied voltage. The emission angle can be steered in the range of  $25^\circ$  by the external voltage. Detailed principles and fabrication methods of the LC-tunable beam steering device have been described in previous publications<sup>14</sup>.

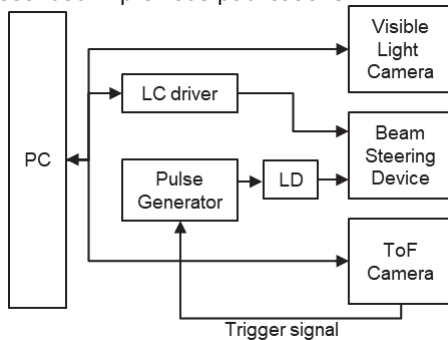


Fig. 2 Schematic of the LiDAR system

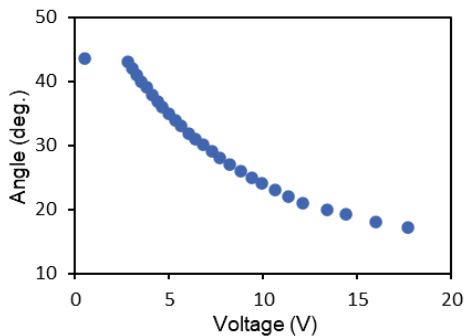


Fig. 3 Emission angle as a function of the applied voltage

## 2.2 Software

The control software consists of three functions: human detection, ranging, and UI control. These functions are DLLs. In the human detection part, the detector of OpenCV, using HoG feature quantity and SVM, performs for the human recognition. A visible light image is captured by a

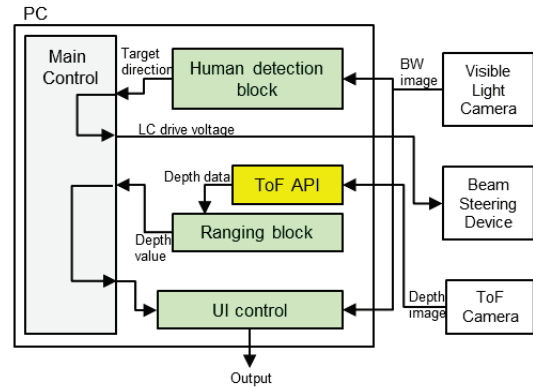


Fig. 4 Schematic of the LiDAR functions

camera, the position of a person in the image is recognized, and the irradiation angle of the laser is calculated from the position. The angle is converted into a liquid crystal driving voltage, and the amplitude value is sent to the liquid crystal driver. The information acquired by the ToF sensor is converted into a ranging image by the software attached to the ToF sensor. The distance measuring part reads it and acquires the distance and direction of the measuring point. A bounding box is drawn at the position of the person in the visible light image, and either of the irradiation angle value or the distance value is overlaid, and it is output with the ranging image. The authors' names should be written in full and center placed just below the title. The name of the presenting author must be underlined.

## 3 Results

### 3.1 Human tracking

A person was made to walk zigzag within the horizontal viewing angle range of the prototype LiDAR. The beam irradiated from the device has a pulse width of 50 ns, a repetition frequency of 10 MHz (duty ratio 50%), and an average power of 1.15 mW. In the present sample, the steering range with practical light quantity was  $24^\circ$ . Figure 4 shows how the prototype LiDAR tracks a person. The bounding box moved according to the movement of the human, and the beam was irradiated tracking the human, and the distance measurement value in the irradiation direction could be obtained. Figure 5 (right) as shown in, when multiple persons were in the field of view, the operation of sequential irradiation of each person was also confirmed.

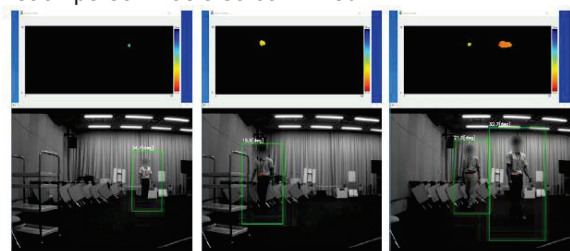


Fig. 5 Human tracking images, ranging images are shown above and visible light images below.

### 3.2 Ranging accuracy

Ranging accuracy was evaluated using a diffusion board as a target. The laser emission angle was fixed near the center of the field of view (voltage 10 V). The pixel with the maximum luminance was selected from the ranging image, and its distance value was used as the distance value to the target. Ten distance measurements were performed at each distance while varying the distance between the target and LiDAR (Fig. 6). The ranging operation was confirmed at the distance of 12 m at the maximum. The dispersion of the measured distance value at the distance of 10 m was 63 mm (0.6%) in the standard deviation and 216 mm (2.1%) in the maximum. The large dispersion in the short distance seems to be caused by the saturation of the incident light power to the image sensor due to the large reflection light power from the target. In the future, it is expected that the measurable distance will be extended by the improvement of beam divergence.

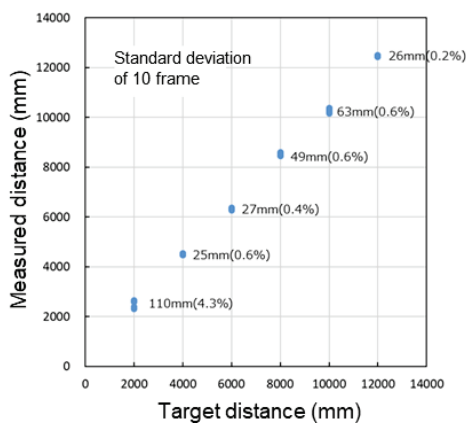


Fig. 6 Ranging results of the LiDAR prototype

### 4 Summary

A prototype of LiDAR using a 1D LC-tunable beam steering device was constructed. By the fusion operation with the visible light camera, it was confirmed that the beam tracked and irradiated the human, and the ranging operation was carried out at maximum 12 m. In this report, it was a two-dimensional measurement, but it can be easily extended to a three-dimensional measurement by using a 2D beam steering device combining a LC-tunable antenna and 1D-OPA. In the future, we will construct a three-dimensional measurable LiDAR and demonstrate ROI ranging operation by it.

### References

[1] Bergman, A. W., Lindell, D. B. and Wetzstein, G., "Deep Adaptive LiDAR: End-to-end Optimization of Sampling and Depth Completion at Low Sampling Rates", Proc. IEEE ICCP, 1-11 (2020)

[2] Lee, M. G., Baeg, S. H., Lee, K. M., Lee, H., Baeg, M. H. Park, J. and Kim, H. K., "Compact 3D LIDAR based on optically coupled horizontal and vertical scanning

mechanism for the autonomous navigation of robots," Proc. SPIE 8037, 80371H (2011).

[3] Hellman, B., Gin, A., Smith, B., Kim, Y. S., Chen, G., Winkler, P., Mccann, P., and Takashima, Y., "Wide-angle MEMS-based imaging lidar by decoupled scan axes" Appl. Opt. 59(1), 28–37 (2020).

[4] McManamon, P. F., Dorschner, T.A., Corkum, D.L., Friedman, L.J., Hobbs, D.S., Holz, M., Liberman, S., Nguyen, H.Q., Resler, D.P., Sharp, R.C. and Watson, E.A., "Optical phased array technology," in Proceedings of the IEEE, 84, 2, 268-298 (1996)

[5] Sun, J., Timurdogan, E., Yaacobi, A., Hosseini, E. S. and Watts, M. R., "Large-scale nanophotonic phased array," Nature 493, 195–199 (2013).

[6] Von Acoleyen, K., Bogaerts, W., Jágerská, J., Thomas, N. L., Houdré, R. and Baets, R., "Off-chip beam steering with a one-dimensional optical phased array on silicon-on-insulator" Opt. Lett. 34, 1477–1479 (2009).

[7] Beeckman, J., Neyts, K. and Vanbrabant, P., "Liquid-crystal photonic applications", Opt. Eng. 50, 081202–081217 (2011).

[8] Yaacobi, A., Sun, J., Moresco, M., Leake, G., Coolbaugh, D. and Watts, M. R., "Integrated phased array for wide-angle beam steering", Opt. Lett. 39, 15 (2014)

[9] Chung, S., Abediasl, H. and Hashemi, H., "A monolithically integrated large-scale optical phased array in silicon-on-insulator CMOS", IEEE J. Solid-State Circuits 53, 275-296 (2018)

[10] Doyle, J. K., Heck, M. J. R., Bovington, J. T., Peters, J. D., Coldren, L. A. and Bowers, J. E., "Two-dimensional free-space beam steering with an optical phased array on silicon-on-insulator", Opt. Express 19, 21595-21604 (2011)

[11] Kwong, D., Hosseini, A., Covey, J., Zhang, Y., Xu, X., Subbaraman, H. and Chen R. T., "On-chip silicon optical phased array for two-dimensional beam steering", Opt. Lett. 39, 941-944 (2014)

[12] Aflatouni, F., Abiri, B., Rekh, A. and Hajimiri, A., "Nanophotonic projection system", Opt. Express 23, 21012-21022 (2015)

[13] Fatemi, R., Khachaturian, A. and Hajimiri, A., "A nonuniform sparse 2-D large-FOV optical phased array with a low-power PWM drive" IEEE J. Solid-State Circuits 54, 1200-1215 (2019)

[14] Kazuki Nakamura, Kenji Narumi, Kohei Kikuchi, Yasuhisa Inada, "Liquid crystal-tunable optical phased array for LiDAR applications," Proc. SPIE 11690, Smart Photonic and Optoelectronic Integrated Circuits XXIII, 116900W (2021)